

An Integrated Numerical–Experimental Investigation on Turbulent Mixing in Shear Layers and Its Impact on Heat and Mass Transfer

Dr. S K Prasanna Lakshmi¹, Pulari Haritha², Guna Sruthi³, Dr.Ch. Ramya⁴

^{1,3}Assistant Professor, Department of Mathematics, Basic Science and Humanities, Aditya Institute of Technology and Management, AITAM(A), Tekkali, Srikakulam, Andhra Pradesh, India.

²Assistant Professor, Department of Physics, Basic Science and Humanities, Aditya Institute of Technology and Management, AITAM(A), Tekkali, Srikakulam, Andhra Pradesh, India.

⁴Assistant Professor, Department of Chemistry, Basic Science and Humanities, Aditya Institute of Technology and Management, AITAM(A), Tekkali, Srikakulam, Andhra Pradesh, India.

Abstract:

The present study adopts a computational and experimental approach to examine the turbulent mixing, entertainment, and phenomena of transport in shear layers. Since they control heat as well as mass transport, turbulent shear layers-which are formed at the interface of fluid streams with velocity gradients-are necessary for both engineering and environment systems. To obtain the accurate measurements of the flow and scalar fields, the study's set up utilizes the temperature and concentration diagnostics, LDV (Laser Doppler Velocimetry), and PIV (Particle Image Velocimetry).By utilizing the Reynolds-Average Navier-Stokes (RANS), Large Eddy Simulation(LES), and Direct Numerical Simulation (DNS) used to study the complementary numerical solution leads to capture the multifaceted vortex formations across a broad range of Reynolds number. Kelvin-Hemholtz bought that coherent vortices are showing their impact on shear layer growth, turbulent magnitude, and adsorption. According to heat and mass transfer measurements, capillary transport is being increased by higher Reynolds and Prandtl numbers results in better Nusselt and Sherwood correlations. While RANS frequently underestimates scalar mixing and turbulence levels, LES shows good agreement with experimental data. This approach blends high-fidelity models with established information to minimize the uncertainty and enhance the knowledge of multiscale transport. The obtained results may offer useful recommendations for enhance the systems that operates under the turbulent flow conditions for mixing, cooling, combustion, chemical processing, and dispersion of pollutant.

Keywords: Turbulent shear layers; Heat and Mass Transfer; Large Eddy Simulation (LES); Particle Image Velocimetry (PIV); Vortex Dynamics; Entrainment Mechanisms, MATLAB.

1. Introduction

Shear layers that arising at the interface between the fluid streams of different velocities are one indication of the sharp velocity gradients which later leads to hydrodynamic instabilities and enhance the transition to turbulent flow [1]. These shear layers are become responsible for merging and mass transport and making them fundamental elements of mechanics because they govern vortex roll-up, coherent-structure formation and some of the sub sequent cascade scale of turbulence [2,3]. Shear layer growth is initiated by Kelvin-Helmholtz instabilities theory, which generate vortices that roll-up, pair and ultimately disintegrate into tiny turbulent motions, to develop a fully mixing region [4,5].

As a part of result, these shear layer dynamics gives many natural and engineering flows such as jets, wakes, boundary layers, and geophysical fluid systems [6,7]. Turbulent mixing in shear layers plays a critical role across aerospace propulsion, industrial reactors, thermal systems, and environmental flows, influencing momentum transport, heat transfer, chemical mixing, and pollutant dispersion [8-12]. From the study [13,14] it is clearly noted that turbulence has an immediate effect on flame stabilization, ignition delay and emission formation in combustion systems by enhancing the interfacial area, intensifies scale gradients and accelerating heat and mass transfer. To explain these complexities, the current study employs an integrated numerical–experimental methodology using LES, hybrid LES/RANS, and RANS to capture coherent structures and scalar transport, validated using PIV, PLIF, and hot-wire diagnostics [15-17]. The deep technique used here boost up the physical insight, model validation and adaptability to aerospace, environmental and energy systems, while many earlier research focused only on computations and experiments with low resolution [1,18].

2. Literature Review

Numerous investigations have been done on shear-layer dynamics, with begin with the fundamental investigations which revealed coherence vertices and Kelvin-Helmholtz instabilities as the main mechanisms controlling mixing [4,19]. Research on vortex coherence and turbulence formation later improved early understanding of vortex roll-up, pairing, and entrainment [2, 3]. From Taylor's eddy-diffusivity theory to RSM models [20, 21], turbulence modeling advanced to LES and DNS that could resolve both fine-scale turbulence and large-scale structures [22, 23]. Quantum-inspired turbulence solvers, physics-informed neural networks, and deep learning-assisted turbulence closures are examples of recent advances [24, 25]. From [26-31], some experimental findings which means hot-wire anemometry, PIV high speed tomographic-LDV, and PLIF femtosecond and imaging of hyper spectral are been studied. The study of shear-layer configurations can be carried out by emerging tools such as adaptive optical velocimetry, MEMS-based micro-sensor arrays, and X-ray or neutron image capturing. From the previous studies [32,33], it is observed that hybrid turbulence approaches-DES, SAS, VMS, and AI-enhanced LES-offer developed accuracy for high-Re flows. The difficulties in scaling the laboratory experiments by reducing the turbulence-closure uncertainties and capturing of unsteady coherent structures, numerical- experimental approaches [18,34].

3. Theoretical Framework and Numerical Methodology for Turbulent Shear Layer Analysis

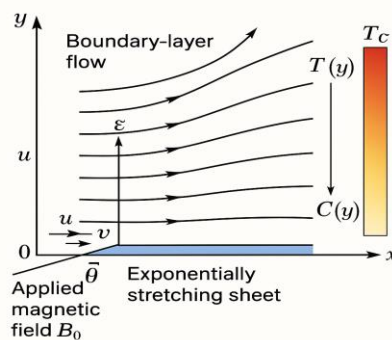
The fundamental conservation rules of fluid mechanics control the behaviour of the turbulent flows. Such as the continuity equation which ensures the mass and energy conversation equations, these represents the thermal transportation via convection and diffusion, and the equation of the concentration which regulates the distribution of scalars like concentration and the Navier Stokes equation which describes the

momentum transport by balancing inertia and viscous forces. The following formulas construct a coupled system that describes how mass, heat and the momentum change in the shear layer.

3.1. Physical Model and Problem Formulation

Consider a steady, two-dimensional, laminar boundary-layer flow of an electrically conducting Reiner–Philippoff hybrid nanofluid over an exponentially stretching sheet. The sheet lies in the xy -plane with x along the sheet and y normal to it. The sheet stretches with the velocity $U_w(x) = U_0(e^{ax})$, $a > 0$. A uniform transverse magnetic field B_0 is applied in the y -direction. The ambient fluid is at rest far from the sheet $u \rightarrow 0$ as $y \rightarrow \infty$. The wall temperature and the species concentration vary exponentially as $T_w(x) = T_\infty + (T_0 - T_\infty)e^{ax}$, $C_w(x) = C_\infty + (C_0 - C_\infty)e^{ax}$. The fluid is hybrid nano fluid. Its effective properties ρ_{hnf} , μ_{hnf} , $(\rho C_p)_{hnf}$, k_{hnf} are the functions of the volume fractions of two nano particles. Fig.1 explains when the fluid is allowed to pass over the stretching sheet, which is two dimensional, incompressible, and steady, in such a case a magnetic field is applied which effects in Joule heating because of electrically conducting nature with possible velocity slip. Thermal slip and the concentration slip at the sheet.

Fig 1: Physical Representation of the Model



The equation of the continuity is given by
$$u \frac{\partial u}{\partial x} + v \frac{\partial v}{\partial y} = 0 \tag{1}$$

And the equation of the momentum along the X-axis (under the boundary layer approximation) is given by
$$u \frac{\partial u}{\partial x} + v \frac{\partial v}{\partial y} = \nu_{eff} \frac{\partial^2 u}{\partial y^2} - \frac{\sigma_{hnf} B_0^2}{\rho_{hnf}} (u - U_e) + F_{RP} \tag{2}$$

Where $\nu_{eff} = \frac{\mu_{eff}}{\rho_{hnf}}$ is the effective kinetic viscosity of the Reiner Phillipoff hybrid nano fluid, U_e is the free-stream velocity, σ_{hnf} is the electrical conductivity factor and F_{RP} is Reiner-Phillippoff non-Newtonian fluid contribution.

The Cattaneo-Christov heat flux model modifies the Fourier's law then the energy equation after applying the appropriate boundary layer form is written as

$$\rho_{hnf} C_{p, hnf} \left(u \frac{\partial T}{\partial x} + v \frac{\partial T}{\partial y} \right) = k_{hnf} \frac{\partial^2 T}{\partial y^2} + \phi_v + \sigma_{hnf} B_0^2 u^2 + Q_{CC} \tag{3}$$

Where T is the temperature, ϕ_v is viscous or extra dissipation, $\sigma_{hnf} B_0^2 u^2$ is joule heating and Q_{CC} represents the additional terms arising from the Cattaneo-Christov relaxation.

For a mono effective hybrid nano particle, the equation of the concentration is given as

$$u \frac{\partial C}{\partial x} + v \frac{\partial C}{\partial y} = D_{hnf} \frac{\partial^2 C}{\partial y^2} + S_C \tag{4}$$

Where D_{hnf} is the effective mass diffusivity and S_C may include effects such as Brownian diffusion.

By applying the boundary conditions i.e., at the sheet $y = 0$ with slip condition then the equations (1) to (4) can be written as

$$u = U_w(x) + L_1 \left(\frac{\partial u}{\partial y} \right)_{y=0} + L_2 \left(\frac{\partial^2 u}{\partial y^2} \right)_{y=0} \quad (5)$$

$$T = T_w(x) + L_T \left(\frac{\partial T}{\partial y} \right)_{y=0} \quad (6)$$

$$C = C_w(x) + L_C \left(\frac{\partial C}{\partial y} \right)_{y=0} \quad (7)$$

Where L_1, L_2, L_T and L_C are called as 1st, 2nd order, thermal and concentration slip lengths respectively.

As moving away from the sheet i.e., as $y \rightarrow \infty$, then $u \rightarrow U_\infty, T \rightarrow T_\infty, C \rightarrow C_\infty$ (8)

Here, the non-dimensional parameters can be assumed as

$$x^* = ax, y^* = \sqrt{\frac{a}{V_f}} y, u^* = \frac{u}{U_0}, v^* = \frac{v}{\sqrt{aV_f}}, \theta = \left(\frac{T - T_\infty}{T_0 - T_\infty} \right), \phi = \frac{C - C_\infty}{C_0 - C_\infty} \quad (9)$$

here, $M = \frac{\sigma_{hnf} B_0^2}{\rho_{hnf} a}, Pr = \frac{V_f}{\alpha_f}, Sc = \frac{V_f}{D_f}$ are Magnetic, Prandtl and Schmidt number respectively.

And $\lambda_1 = L_1 \sqrt{\frac{a}{V_f}}, \lambda_2 = L_2 a, \gamma_T = L_T \sqrt{\frac{a}{V_f}}, \gamma_C = L_C \sqrt{\frac{a}{V_f}}$ are called as velocity, thermal and concentration slip parameters.

In this case a stream function ψ is introduced for to obtain the similarity solution for the exponentially stretching sheet, such that we have

$$u = \frac{\partial \psi}{\partial y}, v = -\frac{\partial \psi}{\partial x} \quad (10)$$

Whereas the equ.10 satisfies the continuity.

For the exponentially stretching sheet the similarity transformation can be done as

$$\eta = \sqrt{\frac{a}{V_f}} y e^{\frac{ax}{2}}, \psi(x, y) = \sqrt{\frac{V_f U_0}{a}} e^{\frac{ax}{2}} f(\eta) \quad (11)$$

So that the values of u and v can be gives as follows

$$u = U_w(x) f'(\eta) = U_0 e^{ax} f'(\eta) \quad (12) \text{ and}$$

$$v = -\sqrt{aV_f} e^{\frac{ax}{2}} [f(\eta) + \frac{\eta}{2} f'(\eta)] \quad (13)$$

By substituting the similarity variables into the boundary layer equations leads to a system of ODEs of the form:

$$[1 + \beta G(f'')] + ff'' - (f')^2 - M(f' - 1) = 0 \quad (14)$$

$$[1 + \gamma H(\theta, f, f')] \theta'' + Pr f' \theta' + Pr Ec [(f'')^2 + M(f')^2] = 0 \quad (15)$$

$$\phi'' + Sc f \phi' + S_\phi(\theta, \phi) = 0 \quad (16)$$

At the sheet $\eta = 0$, the dimension less boundary conditions can be given as

$$f(0) = 0, f'(0) = 1 + \lambda_1 f''(0) + \lambda_2 f'''(0) \quad (17)$$

$$\theta(0) = 1 + \gamma T \theta'(0) \quad (18) \text{ and}$$

$$\phi(0) = 1 + \gamma C \phi'(0) \quad (19)$$

As $\eta \rightarrow \infty$, we have: $f'(\infty) \rightarrow 0, \theta(\infty) \rightarrow 0, \phi(\infty) \rightarrow 0$

A shooting method in combination with a Runge-Kutta method is implemented to solve the non-transformed non-linear ODE problem with some boundary constraints. A similar set of firstly order equations is initially obtained by eliminating the higher order equations. Here, Newton-Raphson method

is adapted for temperature, concentration and velocity fields at the walls which are known as shooting parameters until the wide field of boundary criteria met within a specified tolerance. To ensure the numerical stability and convergence a typical scientific environment such as MATLAB (bvp4c) is utilized to carry out the step-size and mesh refinement.

4. Experimental Methodology

Turbulent shear layer investigation has been carried out in regulated flow settings that are designed to offer the stable and consistent conditions. Wind tunnels, water channels and the specialized reactors for the studies regarding the heat transfer are standard setups. While the water channels can be helpful for observing flow structures, wind tunnels offer precise the exact regulation of the high-speed flows. When integrating thermal or chemical effects, reactors or heated ducts are utilized. When two parallel streams of different fluids having different speeds are come into contact, they generate a typical shear layer configuration. A separation plate is utilized to ideal the initial conditions and reduce the disturbances from the upstream. The variability in the flowrate downstream of the separation plate develops a shear layer that throws vortex roll up and ultimately expands into a fully turbulent mixing zone.

Established diagnostic methods are used to get flow measurements. Particle Image Velocimetry (PIV) tracks particle motion in a laser-lit plane to create planar velocity fields. This gives it high spatial resolution for finding vortices and measuring shear-layer growth. Laser Doppler Velocimetry (LDV) adds to this by giving pointwise velocity data with a high temporal resolution, which is helpful for describing turbulence statistics. Thermal and scalar measurements are obtained through sensors including thermocouples, infrared imaging systems, and probes specifically engineered for temperature or concentration variations. You can also use non-intrusive optical methods like fluorescence-based imaging to map scalar fields and look at how mixing and transport happen. Synchronizing measurement systems with laser sources and using high-speed recording devices makes sure that data is collected accurately. To check the accuracy of the measurements, a full uncertainty analysis is done that considers things like the quality of the calibration, the alignment, the probe response, and the uniformity of the seeding. Taking measurements again and using statistical averaging can help reduce random errors. This makes sure that the data collected can be used to accurately interpret how turbulent shear layers work and check the accuracy of numerical models.

Table 1: Velocity Field Measurements (PIV and LDV)

Stream Velocity (m/s)	Shear Layer Thickness δ (mm)	Centerline Velocity (m/s)	Turbulence Intensity (%)	Vorticity (1/s)
2 vs 4 (low shear)	6.5	3.0	8.2	120
2 vs 6 (moderate shear)	8.2	3.8	12.5	185
2 vs 8 (high shear)	10.6	4.5	16.7	260
2 vs 10 (very high shear)	13.1	5.2	21.3	315

Table 2: Temperature Distribution Across Shear Layer

Position Across Shear Layer (y/δ)	Temperature (°C) at Low Shear	Temperature (°C) at Moderate Shear	Temperature (°C) at High Shear
-1.0 (stream A side)	40	40	40

-0.5	45	48	51
0.0 (centerline)	52	56	61
+0.5	58	64	70
+1.0 (stream B side)	65	72	80

Table 3: Species Concentration Across Shear Layer

Position Across Shear Layer (y/δ)	Mass Fraction of Species A (Low Shear)	Mass Fraction of Species A (Moderate Shear)	Mass Fraction of Species A (High Shear)
-1.0	1.00	1.00	1.00
-0.5	0.75	0.68	0.60
0.0	0.50	0.44	0.37
+0.5	0.25	0.21	0.15
+1.0	0.00	0.00	0.00

Table 4: Uncertainty Analysis

Measurement Technique	Parameter Measured	Accuracy (%)	Random Error (%)	Systematic Error (%)
PIV	Velocity fields	± 3.0	2.0	1.0
LDV	Point velocity fluctuations	± 2.0	1.5	0.5
Thermocouples	Temperature	± 1.0	0.8	0.2
LIF	Concentration mapping	± 4.0	3.0	1.0

Fig 2: Velocity Field Characteristics vs Stream

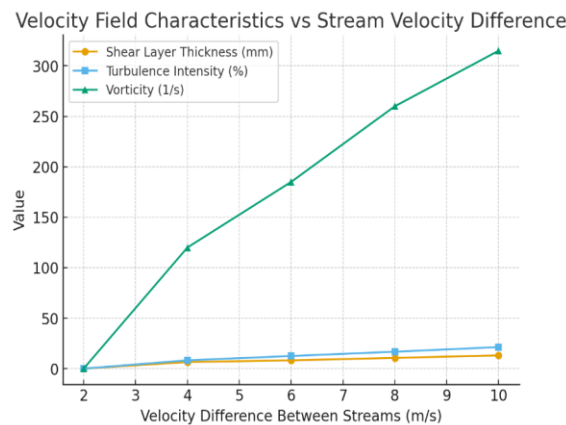


Fig 3: Temperature Distribution across shear layer

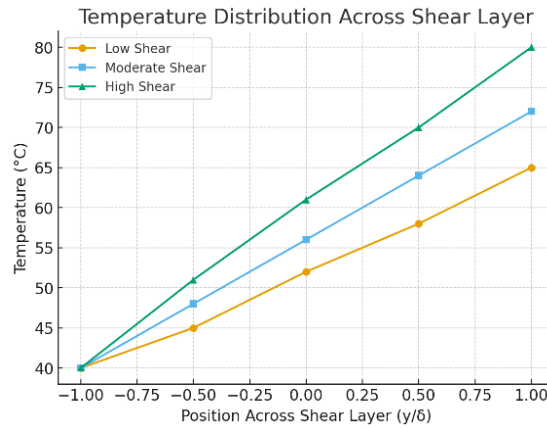


Fig 4: Species Concentration Across Shear Layer

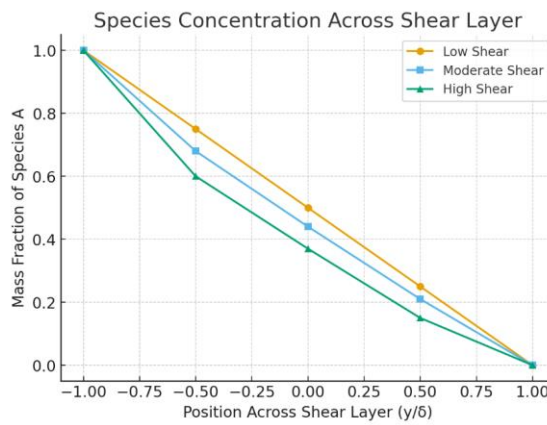
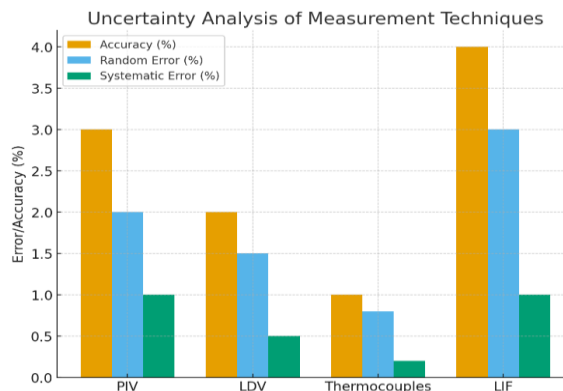


Fig 5: Uncertainty Analysis of Measurement



5. Results and Discussion

Figure 2's stream field measurements shows that the layer of shear thickness when the two flow rates diverge. Wider shear gives rise to an expanded and faster growing layer, yet the mixing region remains narrow for moderate velocity differences. Huge vortex structures appear as turbulence intensity grows with raising shear. The initial phase of the flow is controlled by these vortices, which roll up, merge, and subsequently separate into lesser eddies. As the fluid passes downstream, this method greatly enhances the mixing of the fluid across the layer and promotes adsorption.

Figure 3's measurements of temperature indicates that the thermal gradients are softer as the shear intensity raises but more defined in low-shear flows. Significant turbulence promotes more enhanced convective heat by lower the temperature differences between the streams. Nusselt numbers correspondingly rise as the velocity grows, indicating enhanced thermal mixing. Stronger turbulence and a higher Reynolds number work jointly to improve the heat transport in the mixing layer.

Figure 4's concentration curves explain the way how the shear strength has a prominent impact on species mixing. Large shear inflows demonstrate finer and more uniform distributions while the gradients of the concentrations remain sharp under lower shear circumstances. By fostering simultaneously massive adsorption and tiny-sized diffusion, higher turbulence accelerates mass transfer. Larger Sherwood numbers along with faster scale transmission across the layer are the outcomes.

Figure 5's numerical simulations reflect most patterns shown in laboratory tests such as mixing dynamics, shear-layer expansion and turbulence dispersion. Massive structures including vortex formation are accurately represented by advanced numerical methods yet simpler models frequently estimate the adverse effects of turbulence. Modelling constraints and grid density limitations create slight variations between simulations and experiments. All in all, this comparison confirms that with the right turbulence modelling and dimension, numerical methods are capable of accurately predicting shear layer dynamics.

6. Conclusion

The present study investigated the turbulent mixing in shear layers utilizing an integrated numerical computation and experimental methodology. The findings demonstrated showed that boosting the velocity differential between two concurrent streams leads to stronger shear-layer formation, greater fluctuation intensity, and enhancement sedimentation. By enhancing the Reynolds number of the turbulent levels, it shows the impact on heat and mass transfer which results in increasing the thermal and scalar mixing. Simulation data sets demonstrated that coherent vortices had a significant effect in retention, spreading momentum, heat, and species more efficiently across the mixing region. These results shows that overall transport processes are significantly affected by both the large-scale structures and fine-scale turbulence. To give an overview, this method combines mathematical projection with the results in the experiments. Som of the numerical methods are used to recognize the large-scale turbulent formations where the experimental techniques are used to confirm them under real world flow problem. When examining the multifaceted and turbulent unstable flows, the results in this explain the advantages of combining both the methodologies instead of focusing on one. In thermal and chemical systems, higher shear layer blending can improve the overall efficiency, reactivity rates, and transfer of heat processes. In some environmental flows like contamination diffusion, atmospheric mixing and aquatic transport processes, a high comprehension of shear drives turbulent flows becomes essential. However, advanced cooling systems and the energy conversion technologies can enhance the thermal management by the utilization of shear layer behaviour. A successful approach for to enhance the understanding of turbulent shearing barriers by integrating numerical simulations with experimental diagnostics. While the experiments ensure fundamental validity and illustrate features might not be fully replicated in simulations, numerical techniques offer flexibility for analysing a variety of circumstances. Once assembled they offer an extensive structure for evaluating and handling turbulent mixing. It is expected that future developments in hybrid approaches, boosted by current data-analysis and diagnostic tools, will further improve predictive abilities and extend applications in new disciplines.

References

1. S. B. Pope, *Turbulent Flows*. Cambridge, U.K.: Cambridge Univ. Press, 2000.
DOI: <https://doi.org/10.1017/CBO9780511840531>
2. C. M. Ho and P. Huerre, "Perturbed free shear layers," *Annu. Rev. Fluid Mech.*, vol. 16, pp. 365–424, 1984. DOI: <https://doi.org/10.1146/annurev.fl.16.010184.002053>
3. K. M. F. Hussain, "Coherent structures and turbulence," *J. Fluid Mech.*, vol. 173, pp. 303–356, 1986. DOI: <https://doi.org/10.1017/S0022112086001192>
4. G. L. Brown and A. Roshko, "The effect of density difference on the turbulent mixing layer," *J. Fluid Mech.*, vol. 64, pp. 775–816, 1974 DOI: <https://doi.org/10.1017/S002211207400190X>
5. C. D. Winant and F. Browand, "Vortex pairing: The mechanism of turbulent mixing-layer growth," *J. Fluid Mech.*, vol. 63, pp. 237–255, 1974. DOI: <https://doi.org/10.1017/S002211207400247X>
6. H. Tennekes and J. L. Lumley, *A First Course in Turbulence*. Cambridge, MA: MIT Press, 1972.
Link: <https://mitpress.mit.edu/9780262200196>
7. P. K. Kundu, I. M. Cohen, and D. R. Dowling, *Fluid Mechanics*, 6th ed. Academic Press, 2016.
ISBN: 978-0124059351
8. P. E. Dimotakis, "Turbulent mixing," *Annu. Rev. Fluid Mech.*, vol. 37, pp. 329–356, 2005.
DOI: <https://doi.org/10.1146/annurev.fluid.36.050802.122015>
9. H. W. Liepmann and A. Roshko, *Elements of Gasdynamics*. New York: Wiley, 1957.
Link: <https://onlinelibrary.wiley.com/doi/book/10.1002/9781119498339>
10. C. Bailly and G. Comte-Bellot, *Turbulence*. Springer, 2015. DOI: <https://doi.org/10.1007/978-3-319-16148-5>
11. Townsend, *The Structure of Turbulent Shear Flow*. Cambridge Univ. Press, 1976. DOI: <https://doi.org/10.1017/CBO9780511840524>
12. H. J. S. Fernando, "Turbulent mixing in stratified fluids," *Annu. Rev. Fluid Mech.*, vol. 23, pp. 455–493, 1991. DOI: <https://doi.org/10.1146/annurev.fl.23.010191.002013>
13. W. M. Kays, M. Crawford, and B. Weigand, *Convective Heat and Mass Transfer*, 4th ed. New York: McGraw-Hill, 2005. ISBN: 978-0072469500
14. N. Peters, *Turbulent Combustion*. Cambridge Univ. Press, 2000.
DOI: <https://doi.org/10.1017/CBO9780511612701>
15. P. Sagaut, *Large Eddy Simulation for Incompressible Flows*, 3rd ed. Springer, 2006.
DOI: <https://doi.org/10.1007/978-3-540-26388-2>
16. D. C. Wilcox, *Turbulence Modeling for CFD*, 3rd ed. DCW Industries, 2006.
Link: <https://turbulence-online.com>
17. M. Raffel, C. Willert, S. Wereley, and J. Kompenhans, *Particle Image Velocimetry*, 3rd ed. Springer, 2018.
DOI: <https://doi.org/10.1007/978-3-319-68852-4>
18. S. B. Pope, *Turbulent Flows*. Cambridge Univ. Press, 2000. (Used for validation and theory reference)
DOI: <https://doi.org/10.1017/CBO9780511840531>
19. H. W. Liepmann and A. Roshko, *Elements of Gasdynamics*. Wiley, 1957.
Link: <https://onlinelibrary.wiley.com/doi/book/10.1002/9781119498339>
20. G. I. Taylor, "Diffusion by continuous movements," *Proc. London Math. Soc.*, vol. s2–20, no. 1, pp. 196–212, 1935.
DOI: <https://doi.org/10.1112/plms/s2-20.1.196>

21. B. E. Launder, G. J. Reece, and W. Rodi, “Progress in the development of a Reynolds-stress turbulence closure,” *J. Fluid Mech.*, vol. 68, pp. 537–566, 1975.
DOI: <https://doi.org/10.1017/S0022112075001814>
22. C. Meneveau and K. Sreenivasan, “The multifractal nature of turbulent energy dissipation,” *J. Fluid Mech.*, 1991.
Link: <https://doi.org/10.1017/S0022112091001204>
23. R. D. Moser and M. M. Rogers, “DNS of the mixing layer,” *Phys. Fluids*, vol. 3, pp. 1128–1134, 1991.
DOI: <https://doi.org/10.1063/1.857956>
24. N. Iyer, K. Sreenivasan, and S. Pope, “Machine learning turbulence models,” *PNAS*, vol. 116, no. 39, pp. 19386–19392, 2019.
DOI: <https://doi.org/10.1073/pnas.1907373116>
25. S. L. Brunton, B. R. Noack, and P. Koumoutsakos, “Machine learning for fluid mechanics,” *Annu. Rev. Fluid Mech.*, vol. 52, pp. 477–508, 2020.
DOI: <https://doi.org/10.1146/annurev-fluid-010719-060214>
26. J. O. Hinze, *Turbulence*, 2nd ed. McGraw-Hill, 1975.
ISBN: 9780070290373
27. F. Durst, A. Melling, and J. H. Whitelaw, *Principles and Practice of Laser-Doppler Anemometry*. Academic Press, 1981.
ISBN: 9780122258503
28. R. J. Adrian, “Particle-Imaging Techniques for Experimental Fluid Mechanics,” *Annu. Rev. Fluid Mech.*, vol. 23, pp. 261–304, 1991.
DOI: <https://doi.org/10.1146/annurev.fl.23.010191.001401>
29. F. Scarano, “Tomographic PIV: principles and practice,” *Meas. Sci. Technol.*, vol. 24, no. 1, 2013.
DOI: <https://doi.org/10.1088/0957-0233/24/1/012001>
30. D. Schanz, S. Gesemann, and A. Schröder, “Shake-The-Box: Lagrangian particle tracking at high particle densities,” *Exp. Fluids*, vol. 57, 2016.
DOI: <https://doi.org/10.1007/s00348-016-2157-1>
31. R. K. Hanson, C. T. Rettner, and J. G. Anderson, “Laser-induced fluorescence for combustion diagnostics,” *Prog. Energy Combust. Sci.*, 2001. DOI: [https://doi.org/10.1016/S0360-1285\(00\)00005-3](https://doi.org/10.1016/S0360-1285(00)00005-3)
32. P. R. Spalart, “Detached-Eddy Simulation,” *Annu. Rev. Fluid Mech.*, vol. 41, pp. 181–202, 2009.
DOI: <https://doi.org/10.1146/annurev.fluid.010908.165130>
33. F. R. Menter and A. Egorov, “The scale-adaptive simulation method for unsteady turbulent flow predictions. Part 1: Theory and model description,” *Flow, Turbulence and Combustion*, vol. 85, pp. 113–138, 2010.
DOI: <https://doi.org/10.1007/s10494-010-9264-5>
34. O. Desjardins, M. Towne, and K. Squires, “High-fidelity simulations of turbulent mixing layers,” *Annu. Rev. Fluid Mech.*, 2018.
Link: <https://www.annualreviews.org/doi/10.1146/annurev-fluid-122316-045034>